Chapter 11
Interperiods Electron Transport Coherences in Quantum-Cascade Structures

Mykhailo V. Klymenko, Oleksiy V. Shulika, Igor A. Sukhoivanov

Abstract Results of electron transport investigation in the quantum-cascade structures are reported. Mathematical model connecting optical characteristic and electron transport have been developed applying the density matrix theory. It is shown that series of electron coherent transitions in the injector influence on the optical response of the quantum-cascade structure.

11.1 Introduction

Up to date, many efforts have been made to investigate the interplay between optical and transport processes that is crucial for understanding the optical response of the quantum-cascade structures (QCS) [1–6]. Recently, special attention has been paid to the effect of coherent electron transport in QCS [3–6]. Published in Refs. [5, 6], results of the pump-probe experiments have shown oscillatory behavior of the optical response of terahertz GaAs/$Ga_{0.15}Al_{0.85}As$ QCS at femtosecond time intervals. Applying density matrix formalism, such a behavior of optical characteristics was explained in Ref. [5] as due to coherent transition of electrons between the injector and active region through the injection barrier. The effect is strongly depended on the width of the injection barrier layer. Also, oscillating behavior of the optical response have been observed in the mid-infrared $In_{0.61}Ga_{0.39}As/In_{0.45}Al_{0.55}As$ QCS which has more complicated injector containing many quantum states [7, 8]. In this work, we show that the optical response of such structures is affected not only by the coherent electron transport through the injection barrier between the active region

Mykhailo V. Klymenko, Oleksiy V. Shulika
Kharkov National University of Radio Electronics, Lenin ave. 14, Kharkov 61166, Ukraine,
e-mail: klymenko@daad-alumni.de

Igor A. Sukhoivanov
Department of Electronics Engineering, DICIS, University of Guanajuato, Mexico,
e-mail: i.sukhoivanov@ieee.org

M.F. Pereira and O. Shulika (eds.), *Terahertz and Mid Infrared Radiation*: *Generation, Detection and Applications*, NATO Science for Peace and Security Series B: Physics and Biophysics, DOI 10.1007/978-94-007-0769-6_11,

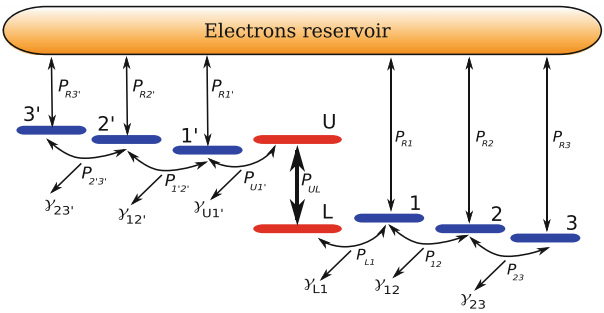

Fig. 11.1 Diagram of localized states chosen as a basis states for density matrix of the QCS. Optical transitions proceed between states U and L. States 1, 2 and 3 belong to the left injector. The right injector contains states $1'$, $2'$ and $3'$. The structure is terminated by reservoirs at both ends

and first nearest state in the injector, but also by many other coherent passages between states in injectors. An evidence of such complicated coherences follows from spreading of the Wanier-Stark wave function through several quantum wells [9]. The stationary Wannier-Stark state can be represented as a superposition of several localized basis functions which are not eigenstates of the Hamiltonian for the QCS. In this case, amplitude variations of any localized state lead to coherent sequential tunneling between all localized state. Here, we intend to answer the question how many states in the injector have strong influence on the optical interactions in the active region. To realize that, we provide mathematical modeling of pump-probe experiments.

11.2 Density Matrix

11.2.1 General Properties of the Density Matrix for the Quantum-Cascade Structures

As an example, we consider the mid-infrared $In_{0.61}Ga_{0.39}As/In_{0.45}Al_{0.55}As$ quantum-cascade structure. Usually, the coherent transport is treated applying the density matrix theory [10]. This theoretical tool allows to consider the interplay between coherent transport and many-body effects as well as non-linear optical effects. In this work, we have chosen the eigenstates of uncoupled quantum wells as basis functions for the density matrix [4]. The energy of the basis states are shown in Fig. 11.1 schematically. To estimate the contribution of coherences in the injector, we compute the optical response for several models having different configurations of the energy states. Namely, we consider $(R-1'-U-L-1-R)$, $(R-2'-1'-U-L-1-2-R)$ and $(R-3'-2'-1'-U-L-1-2-3-R)$ chains of states (see Fig. 11.1). Indices contain two quantum numbers which are the subband number and in-plane-wave vector.

The density matrix derived here has the structure represented in Fig. 11.2. The matrix have tree diagonals, because only sequential electron transitions are under consideration. All other transitions are neglected.

The Hamiltonian of the QCS can be represented as follows [10]:

$$H = \sum_j H_j + \sum_{j,i \neq j} H_{ij} \tag{11.1}$$

The term H_j describes kinetic energy, all vertical transitions and scattering events in the j quantum well. The explicit expression for the first term is taken from [5]. Hereafter, we consider many-body effects at the Hartree-Fock level of approximations. Higher-order correlations are treated phenomenologically using dephasing times and electron lifetimes. Dephasing in the active region is equal 20 meV [8]. Lifetimes for lasing subbands have been taken as 0.2 ps [9]. Scatterings in the injector are described by own dephasing times. We assume that most scattering events occur in the active region. Therefore, for subbands in the injector, these values are $\gamma_{ij} = 5$ meV, $\tau_j = 3$ ps. Second sum in (11.1) describes coherent tunneling energy. This term appears due to non-stationarity of the basis functions. In the second-quantization formalism, it is given by $H_{ij} = \mu_{ij} a_i^\dagger a_j + \mu_{ji} a_j^\dagger a_i$. Here, μ_{ij} is the coupling strength. $a_i^\dagger$ is the creation operator, and a_i is the annihilation operator. The coupling strength is proportional to the overlap integral of basis functions [10]. This term allow to consider resonant tunneling as well as off-resonant one.

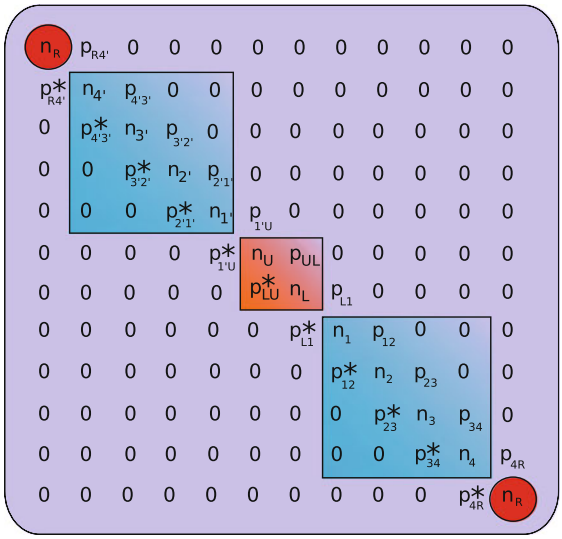

Fig. 11.2 Structure of the density matrix for 1.5 periods of the QCS terminated by electron reservoirs. Matrix elements in the orange square describe transport processes in the active region. Matrix elements in the blue squares correspond to the injector states. Red circles contains density matrix elements for reservoirs

11.2.2 Kinetic Equations

To derive the time evolution of observables, it is necessary to solve the system of Liuville-von-Neuman equations for density matrix elements. After evolution of all commutators in right-hand side of Liuville-von-Neuman equations, one gets following system of equations:

$$\dot{p}_{j,j+1} = i\omega_{j,j+1}p_{j,j+1} + i\mu_{j,j+1}(n_j - n_{j+1})/\hbar + \gamma_{j,j+1}p_{j,j+1} \tag{11.2}$$

$$i\hbar\dot{n}_j = Im\left[\mu_{j,j+1}p_{j,j+1}\right] - Im\left[\mu_{j,j-1}p_{j,j-1}\right] - (1/\tau_j)(n_j - n_j^{stat}) \tag{11.3}$$

where: $j = R, 3', 2', 1', U, L, 1, 2, 3, R$; $j+1$ denote next index after j in the series of states; $\omega_{j,j+1}$ is the frequency of the electron transition; $p_{j,j+1}$ is the off-diagonal density matrix element; $n_{j,j+1}$ is the diagonal density matrix element; $\mu_{j,j+1}$ is the coupling strength; $\gamma_{j,j+1}$ is the dephasing time; τ_j is the electron lifetime.

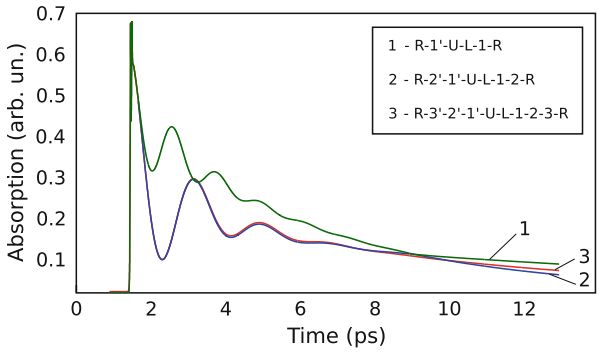

Fig. 11.3 Computed pump-probe optical response of the QCS for different numbers of states in the injector. Each curve corresponds to some defined path of electrons through states shown in Fig. 11.1

In the non-equilibrium regime, quantum dynamics of observables is very sensitive to the initial conditions. In this paper, we prepare the system in the Wannier-Stark state at the initial time. The Wannier-Stark states are solutions the stationary Schrodinger equation with the potential profile of the QCS. The coherent transport without scattering at an external particle is forbidden between Wannier-Stark states due to their orthogonality. However, such a transport is possible if some changes have been brought to the system making initial states be non-stationary. In our case, such a change is caused by pump optical pulse.

11.3 Interpretation of Pump-Probe Experiments

We apply the theory developed above to modeling of the pump-probe optical response of QCS. The pump-probe experiments are based on third-order non-linear optical effects. In this paper, we get the non-linear optical response of third order using sequential computations of microscopic polarization of each order beginning from zero one up to the fourth order. Detailed description of such an iterative procedure can be found in Ref. [11] (p. 95). The results of pump-probe experiment modeling is presented in Fig. 11.3. As follows from results, inclusion into consideration states 2 and $2'$ leads to significant modification of the characteristics. Contribution from the states 3 and $3'$ is not so significant. In this case, some kind of convergence is observed. Thus, the correct prediction of pump-probe optical response for considered structure can be realized considering only two states in the injector. In general case, this number is depended on the following factors:

1. Coherent coupling between states which is defined by the overlap integral of their wave functions
2. Energy gap between energy states (resonant or off-resonant tunneling)
3. Lifetime of the electron states
4. Dephasing time for the coherent transport between states

First two factors are dependent on the band structure and wave functions of the injector. Other parameters reflect a manifestation of many-body effects. The exponential decay of the optical absorption is caused by the finite lifetime of electrons at laser states. The period of oscillations is defined by the injector design mainly.

The results are evidence of significant influence of deeper states of the injector on the optical response in the active region. Therefore, accurate modeling of pump-probe experiments require consideration of many coherent transport processes inside injectors. Also, the convergence of results have been observed after inclusion into consideration some defined number of subbands in the injector.

Acknowledgements This work is partially supported by the project of the University Guanajuato, Mexico #000015/08 and #000030/09.

References

[1] Lee S.C., Wacker A.: Nonequilibrium Green's function theory for transport and gain properties of quantum cascade structures. Phys. Rev. B **66**, 245314-1-18 (2002)
[2] Waldmueller I., Chow W.W., Young E.W., Wanke M.C.: Nonequilibrium many-body theory of intersubband lasers. IEEE J. Quantum Elec. **42**, 292-301 (2006)
[3] Iotti R.C., Rossi F.: Nature of Charge Transport in Quantum-Cascade Lasers. Phys. Rev. Lett. **87**, 146603-1-4 (2001)
[4] Callebaut H. and Hu Q.: Importance of coherence for electron transport in terahertz quantum cascade lasers. J. Appl. Phys. **98**, 104505-1-11 (2005)

[5] Weber C., Wacker A., Knorr A.: Density-matrix theory of the optical dynamics and transport in quantum cascade structures: The role of coherence. Phys. Rev. B *79*, 165322-1-14 (2009)
[6] Weber C., Banit F., Butscher S., Knorr A., Wacker A.: Theory of the ultrafast nonlinear response of terahertz quantum cascade laser structures. Appl. Phys. Lett. **89**, 091112-1-3 (2009)
[7] Kuehn W., et al: Ultrafast phase-resolved pump-probe measurements on a quantum cascade lasers. Appl. Phys. Lett. **93**, 151106 1-3 (2008)
[8] Choi H., et al: Femtosecond dynamics of resonant tunneling and superlattice relaxation in quantum cascade lasers. Appl. Phys. Lett. **92**, 122114 1-3 (2008)
[9] Faist G., Beck M., Aellen T., Gini E.: Quantum-cascade lasers based on bound-to-continuum transitions. Appl. Phys. Lett. **78**, 147 1-3 (2001)
[10] Meier, T., Thomas, P., Koch, S.W.: Coherent Semiconductor Optics: From Basic Concepts to Nanostructure Applications. Springer, New York (2007)
[11] Schafer, W., Wegener, M.: Semiconductor optics and transport phenomena. Springer, Berlin (2002)